J Solid State Electrochem (1998) 2: 211–215

ORIGINAL PAPER

Satoru Yamamura · Hiromichi Koshika
Matsuhiko Nishizawa · Tomokazu Matsue
Isamu Uchida

In situ conductivity measurements of $LiMn_2O_4$ thin films during lithium insertion/extraction by using interdigitated microarray electrodes

Received: 17 June 1997 / Accepted: 2 January 1998

Abstract Thin films of $LiMn_2O_4$ have been prepared by RF magnetron sputtering on interdigitated microarray electrodes. In situ conductivity–potential profiles and cyclic voltammograms during extraction/insertion processes of Li ions were obtained simultaneously in nonaqueous and aqueous electrolyte solutions (1 M $LiClO_4$/propylene carbonate and 1 M LiCl/water). The electronic conductivity of $Li_{1-x}Mn_2O_4$ was found not to show metallic transition and maintain its semiconducting state during the extraction/insertion of Li ion. A slight decrease in conductivity was observed with increasing the anodic potential, i.e., with increasing x (lithium extraction) and recovered reversibly when the potential returned to the cathodic side (re-insertion of Li ions). Similar results were obtained in both aqueous and nonaqueous electrolyte solutions.

Key words Spinel-type $LiMn_2O_4$ · Interdigitated microarray electrodes · In situ conductivity measurements · Semiconductor electrode · Li ion battery

Introduction

In recent years, much interest has centered on the search for lithium insertion electrodes for lithium secondary batteries, because lithium rechargeable batteries with high energy density have been recognized as indispensable devices in high-performance, portable electronic equipment. Various kinds of transition metal oxides and sulfides that accommodate lithium ions by topotactic reaction have been studied as candidates [1, 2]. Although $LiCoO_2$ is being used as the cathode of commercial products [3], spinel manganese oxide is strongly attractive because of its cost performance. Manganese is more abundant and much less expensive than cobalt. There are many studies on $Li_{1-x}Mn_2O_4$, which has been characterized by electrochemical and X-ray diffraction methods [4–8].

Thin films of transition metal oxide are also of interest in the fields of all solid-state microbatteries [9, 10] and electrochromic devices [11]. Fabrication of $LiMn_2O_4$ thin film has been reported using various techniques, for example, spray pyrolysis [12], chemical vapor deposition [13], electron beam evaporation [14], RF magnetron sputtering [15], pulsed laser deposition [16], and thermal decomposition [17].

The conductivity is an important property in the design of high-performance batteries. $LiMn_2O_4$ is categorized as a hopping semiconductor, and its conductivity has been measured extensively [17–19]. The electronic conduction of transition metal oxide is related to d electrons, whose properties vary widely from insulating to metallic via semiconductivity. The properties of d electrons in these compounds are influenced by nonstoichiometry. Indeed, lithium-deficient $Li_{1-x}CoO_2$ causes metal-insulator transition [20, 21]. Pistoia et al. investigated the resistance of $Li_{1-x}Mn_2O_4$ by impedance measurements [19]. However, the a.c. impedance method yields the conductivity in the direction from the electrode toward the solution. In contrast, the in situ method reported here with an interdigitated microarray (IDA) electrode provides the conductivity in the lateral direction. We applied this technique to investigate the conductivity of polypyrrole [22, 23], fullerene [24], $Li_xV_2O_5$ [25], and $Li_{1-x}CoO_2$ [21], since this method gives the intrinsic conductivities as a function of x in the whole potential region accessible in a particular electrolytic solution, simultaneously with a cyclic voltammogram.

In this paper, we report the fabrication and characterization of $Li_{1-x}Mn_2O_4$ thin films on IDA electrodes on silicon substrates. The initial film of $LiMn_2O_4$ was prepared by RF magnetron sputtering, and the spinel structure was obtained by annealing at 700 °C.

S. Yamamura · H. Koshika · M. Nishizawa
T. Matsue · I. Uchida (✉)
Department of Applied Chemistry,
Graduate School of Engineering,
Tohoku University, Aramaki-Aoba,
Aoba-ku, Sendai 980-77, Japan

Electrochemical and electric properties of the thin film were investigated simultaneously by cyclic voltammograms and in situ conductivity measurements.

Experimental

The IDA electrode and the electrochemical apparatus for the in situ conductivity measurements used in this work were similar to those described previously [21, 25]. The IDA electrode was fabricated by photolithography with a sputter-deposited Pt film on a thermally oxidized silicon wafer substrate. The IDA electrode has two sets of comb-type Pt arrays; each array has 50 electrode elements, 0.1 μm thick, 10 μm wide, and 2.4 mm long, separated by 10 μm from its adjacent elements (Fig. 1). The lead part of the IDA electrode was insulated with an SiO_2 film.

$LiMn_2O_4$ was deposited by RF magnetron sputtering of $LiMn_2O_4$ onto the IDA electrode. The target was prepared by sintering a mixture of $LiMn_2O_4$ powder and polyethylene glycol (1 wt %) as a binder at 880 °C in air for 12 h. The diameter of the target was 3 in. The $LiMn_2O_4$ powder was prepared by the solid-state reaction of a stoichiometric mixture of $LiOH{\cdot}H_2O$ and MnO_2 at 800 °C in air for 24 h. Sputtering was carried out through an aluminum mask in 0.02 torr of a 10/1 Ar/O_2 mixture with 100 W RF power, and the substrate temperature was kept at 100–120 °C during deposition. After sputtering for 50 min, 0.2 μm thickness was obtained (40 Å/min), as determined by a surface texture analyzer (Dektak 3030ST). The as-deposited film shows no crystallinity, but the definite crystal structure peculiar to spinel was restored as shown in Fig. 2, by annealing at 700 °C in O_2 for 1 h. The X-ray diffraction was obtained by a Shimadzu XD-D1 X-ray diffractometer using CuK_α radiation.

The electrochemical measurements were carried out on annealed films of $LiMn_2O_4$ in 1 M $LiClO_4$/propylene carbonate (PC) solutions in an Ar-filled dry box (Miwa MDB-1B + MS-P15 S). The water content of the PC solution used was <20 ppm. Li foil was used for the reference and counter electrodes.

The electrical conductivity of the film was determined from the current which flows between the two sets of working electrodes (W1, W2). The potentials of W1 and W2 were controlled by means of a bipotentiostat with a potential difference (5 or 10 mV) between them, and the film conductivity was calculated from the ohmic current flowing through the film via the two working electrodes by using the following equation [19]

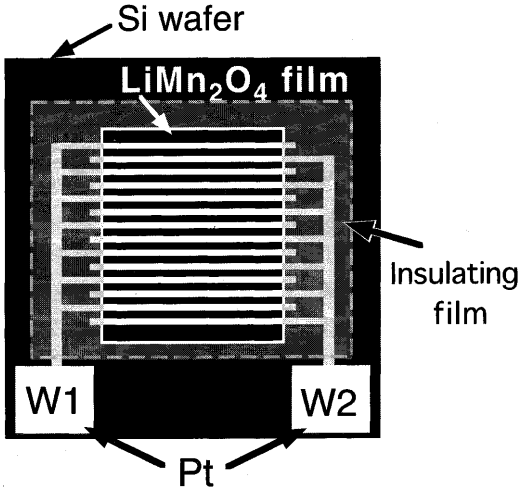

Fig. 1 A schematic representation of the IDA for in situ conductivity measurements: electrode width 10 μm, length 2.4 mm, 50 elements

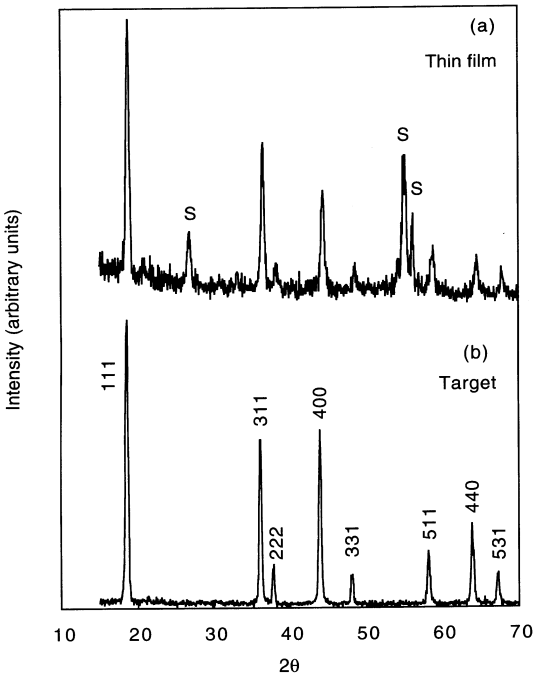

Fig. 2 X-ray diffraction patterns of *a* $LiMn_2O_4$ thin film annealed at 700 °C and *b* the target material. Diffraction lines of the SiO_2 substrate are marked "S"

$$\sigma = I_\Omega w/2ld \text{ V S/cm} \quad (1)$$

where i_Ω is the ohmic current, w the gap width of arrays, l the total length of electrode, d the thickness of film, and V the potential difference between arrays. The ionic conductivity of electrolyte solutions is negligible in this d.c. method.

Steady-state conductivity measurements were also carried out. After a fixed amount of Li insertion/extraction was performed electrochemically at a constant current, the IDA electrode was disconnected from the current source and left at open circuit for a while until its potential reached a steady state. Then, a constant potential difference was applied between W1 and W2 and the current flow was measured using a source measure unit (Keithley 236). All the measurements were carried out at 25 °C.

Results and discussion

Figure 2a shows the X-ray diffraction pattern of $LiMn_2O_4$ film prepared on the oxidized silicon substrate by sputtering and postannealing at 700 °C compared with that of $LiMn_2O_4$ spinel used as a target material (Fig. 2b). The peaks marked "S" are due to the SiO_2 substrate. The other peaks were all attributed to $LiMn_2O_4$ spinel [26], and the crystallinity of the film was confirmed. From SEM observations (not shown), the annealed film was found to be made up of grains of ca. 1 μm diameter.

Figure 3 shows a typical cyclic voltammogram (a) and an in situ potential–conductivity profile (b) of $Li_{1-x}Mn_2O_4$ film annealed at 700 °C taken simultaneously at a scan rate of 0.1 mV/s. No drastic change in conductivity such as metallic transition was observed,

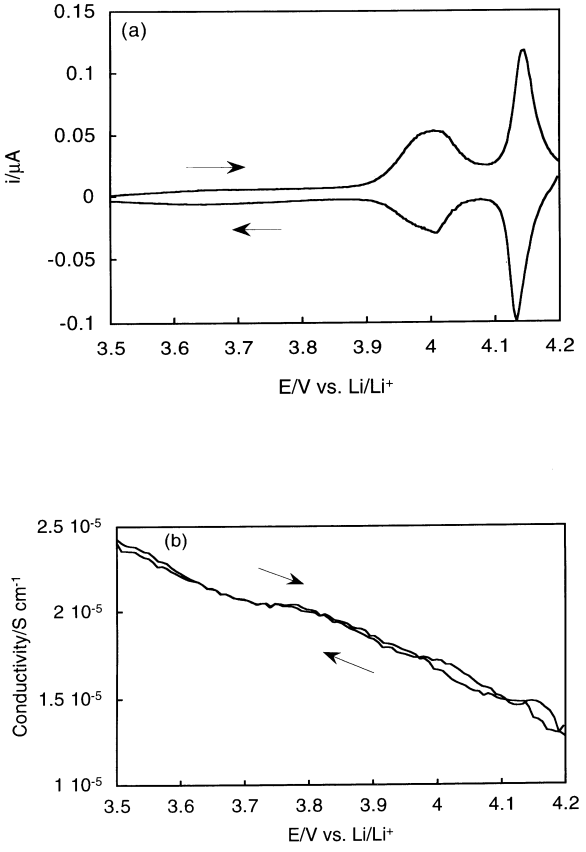

Fig. 3 Cyclic voltammogram (**a**) and potential–conductivity profile (**b**) of a 0.2-μm thick $LiMn_2O_4$ film annealed at 700 °C, obtained in 1 M $LiClO_4$/PC by in situ measurement using IDA: scan rate 0.1 mV/s, potential difference between arrays 5 mV

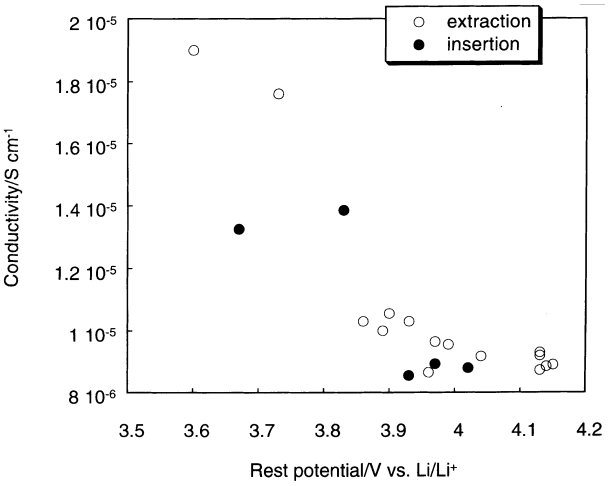

Fig. 4 The rest potential–conductivity profile of a 0.2 μm thick $LiMn_2O_4$ film annealed at 700 °C, taken in 1 M $LiClO_4$/PC after Li extraction/insertion. Applied potential between arrays of IDA 5 mV

while the conductivity decreased monotonically during Li extraction within the order of 10^{-5} S/cm. There are two current peaks observed in the cyclic voltammogram (CV) with anodic potential scanning, but no corresponding–conductivity change was observed in the potential region. The potential-conductivity profile showed good reversibility, and gave reproducible results under successive scans.

It is not certain that the nonstoichiometry (x in $Li_{1-x}Mn_2O_4$) was changed for the whole of the film by the potentiodynamic method used above. Thus, in order to confirm the data obtained under potentiodynamic conditions, steady-state measurements were also carried out. A known amount of charge was applied with a constant current, and the conductivity of the film was measured after the open circuit potential reached a steady value. Figure 4 shows a steady-state potential–conductivity profile of an annealed $Li_{1-x}Mn_2O_4$ film, being in agreement with the profile obtained in the potentiodynamic condition. With increasing x value (extraction of Li^+), the electronic conductivity of $Li_{1-x}Mn_2O_4$ decreased gradually and recovered reversibly by re-insertion of Li^+. We also measured the solid-state electrical conductivity of a $LiMn_2O_4$ pellet made of the powdered material by a two-probe d.c. method, and obtained 3.2×10^{-5} S cm^{-1} at 25 °C, which is in the range of reported values (10^{-4}–10^{-6} S/cm) in the literature [17–19]. It can be seen that the values noted at the most positive potential (~3.5 V vs Li/Li^+) in the potential–conductivity profiles showed almost the same value as the solid state conductivity value of $LiMn_2O_4$ ($x = 0$ in $Li_{1-x}Mn_2O_4$).

It is said that $Li_{1-x}Mn_2O_4$ spinel is a mixed-valence (Mn^{3+}/Mn^{4+}) compound and its electronic conduction takes place by electron hopping between high-valence and low-valence states. However, some lithium spinels, $LiTi_2O_4$ and LiV_2O_4, are reported to have metallic conductivity [18]. In the case of $Li_{1-x}CoO_2$ [21], the conductivity increases rapidly with increasing anodic potential during the change $0 < x < 0.1$ and reaches a saturated value, indicating an insulator–metal transition. According to Goodenough [27], a metal–insulator (semiconductor) transition may occur in the oxides of transition metals of the octahedral configuration when the metal–metal distance becomes less than the critical distance (R_C); R_C for $LiMn_2O_4$ is 2.743 Å [19]. Pistoia et al. reported that metallic transition does not occur for $LiMn_2O_4$, because the R_C value is much lower than the $R_{Mn\text{-}Mn}$ for $LiMn_2O_4$ (2.913 Å) and for the fully delithiated spinel (2.830 Å) [19]. Our results for $Li_{1-x}Mn_2O_4$ also do not show transition from the semiconductor to the metallic state, supporting their observation. Considering that the conductivity decreases with increasing anodic potential, we can say that this behavior resembles the potential dependence of surface conductance in the electron-depleted space charge region for n-type semiconductors [28, 29].

Recently, lithium insertion in $LiMn_2O_4$ was demonstrated from an aqueous electrolyte [30]. It has been shown that $LiMn_2O_4$ placed in aqueous solutions undergoes an electrochemical topotactic reaction,

$$Li_{1-x}Mn_2O_4 + xLi^+ + xe^- \rightarrow LiMn_2O_4 \qquad (2)$$

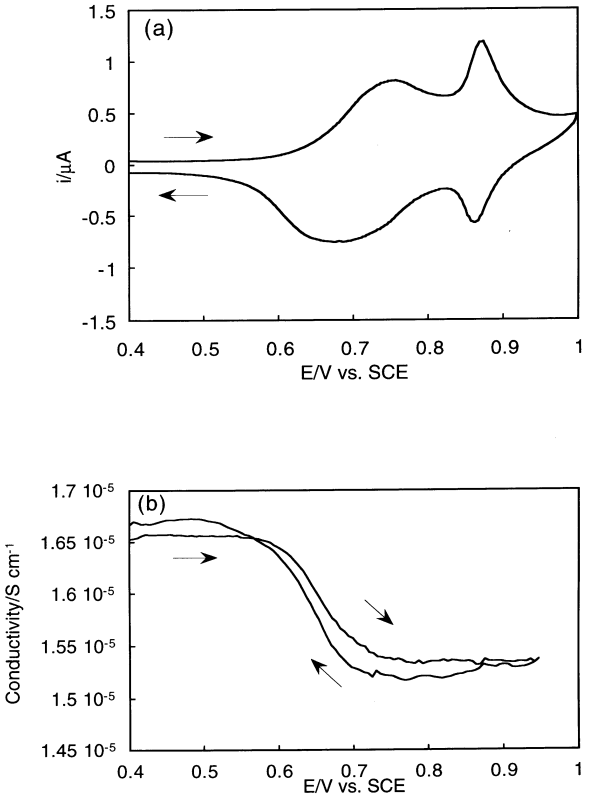

Fig. 5a, b Cyclic voltammogram (**a**) and potential-conductivity profile (**b**) of a 0.2-μm thick $LiMn_2O_4$ film annealed at 700 °C, obtained in 1 M LiCl by in situ measurement using IDA: scan rate 1 mV/s, potential difference between arrays 5 mV

The electrochemical insertion/extraction reaction of lithium ion with $LiMn_2O_4$ in aqueous solutions has been studied from the standpoint of the development of rechargeable lithium-ion cells with aqueous electrolytes [30], lithium ion-selective electrode [31], and electrochromic devices [32].

In situ conductivity measurements in an aqueous electrolyte were also carried out here. Figure 5 shows a cyclic voltammogram (a) and an in situ potential–conductivity profile (b) of an annealed $LiMn_2O_4$ film at the IDA electrode in a 1 M LiCl aqueous solution, where a saturated calomel electrode and a Pt wire were used as reference and counter electrode respectively. The voltammogram shows two peaks for both the forward and reverse scans, and shows good reversibility. This indicates that electrochemical insertion/extraction of Li with $LiMn_2O_4$ can take place in LiCl solutions. The conductivity decreases with extraction of Li^+ and increases with insertion of Li^+, while this change was only 0.1×10^{-5} S/cm. There was no irreversible change observed within 10 cycles.

The conductivity of $Li_{1-x}Mn_2O_4$ decreased toward the anodic direction with decreasing lithium content in the spinel. This apparent behavior of potential dependence is similar to that of the surface conductivity of n-type semiconductors, which can be explained by the space charge layer effect [28, 29]. However, preliminary tests for plots of the observed conductivity against $E^{-1/2}$ (or E^{-1}) did not show significant linear relationships. In addition, regarding the conductivity profile and the degree of conductivity change, an evident difference was recognized when we changed the kinds of electrolyte solutions (aqueous and non-aqueous). Continuous change in nonstoichiometry (x in $Li_{1-x}Mn_2O_4$), anion adsorption at the surface, and the space charge property may be correlated to each other. Further studies including the photo effect are under way in this laboratory to understand the details.

Conclusions

In situ conductivity–potential profiles and cyclic voltammograms of $LiMn_2O_4$ during Li^+ ion insertion/extraction processes were measured simultaneously by using an IDA electrode technique in nonaqueous and aqueous electrolytes. Lithium extraction from $LiMn_2O_4$ causes no metallic transition and maintains the semiconducting state, in contrast to the metallic transition we reported previously for $LiCoO_2$ [21]. The conductivity of $LiMn_2O_4$ slightly decreases during Li^+ ion extraction in the anodic scan and returns to its original value during the re-insertion. In conclusion, the present study has demonstrated that in situ conductivity measurements using an IDA electrode technique are useful for characterizing the conductivity change in nonstoichiomety caused by the lithium ion extraction/insertion process of the battery active materials.

Acknowledgements This work was supported partly by The Osaka Science & Technology Center and partly by a Grant-in-Aid for Scientific Research on the Priority Area of "Electrochemistry of Ordered Interfaces" (No. 09237212) from the Ministry of Education, Science, Sports and Culture, Japan.

References

1. Scrosati B (1994) In: Lipkowski J, Ross PN (eds) Electrochemistry of novel materials. VCH, Weinheim, pp 111–140
2. Pistoia G (ed) (1994) Lithium batteries, new materials, developments and perspectives. Elsevier, Amsterdam
3. Ozawa K (1994) Solid State Ionics 69: 212
4. Thackeray MM, David WIF, Bruce PG, Goodenough JB (1983) Mater Res Bull 18: 461
5. Thackeray MM, Johnson PJ, Picciotto LA, Bruce PG, Goodenough JB (1984) Mater Res Bull 19: 179
6. David WIF, Thackeray MM, Picciotto LA, Goodenough JB (1987) J Solid State Chem 67: 316
7. Ohzuku T, Kitagawa M, Hirai T (1990) J Electrochem Soc 137: 769
8. Yamada A, Miura K, Hinokuma K, Tanaka M (1995) J Electrochem Soc 142: 2149
9. Antaya M, Dahn JR, Preston JS, Rossen E, Reimers JN (1993) J Electrochem Soc 140: 575
10. Wang B, Bates JB, Hart FX, Sales BC, Zuhr RA, Robertson JD (1996) J Electrochem Soc 143: 3203
11. Wei G, Haas TE, Goldner RB (1992) Solid State Ionics 58: 115
12. Fragnaud P, Schleich DM (1995) Sens Actuators A51: 21

13. Fragnaud P, Nagarajan R, Schleich DM, Vujic D (1995) J Power Sources 54: 362
14. Shokoohi FK, Tarascon JM, Wilkens BJ, Guyomard D, Chang CC (1992) J Electrochem Soc 139: 1845
15. Hwang KH, Lee SH, Joo SK (1994) J Electrochem Soc 141: 3296
16. Striebel KA, Deng CZ, Wen SJ, Cairns EJ (1996) J Electrochem Soc 143: 1821
17. Kanoh H, Feng Q, Hirotsu T, Ooi K (1996) J Electrochem Soc 143: 2610
18. Schutte L, Colsmann G, Reuter B (1979) J Solid State Chem 27: 227
19. Pistoia G, Zane D, Zhang Y (1995) J Solid State Chem 142: 2551
20. Molenda J, Stoklosa A, Bak T (1989) Solid State Ionics 36: 53
21. Shibuya M, Nishina T, Matsue T, Uchida I (1996) J Electrochem Soc 143: 3157
22. Nishizawa M, Sawaguchi T, Matsue T, Uchida I (1991) Synth Met 45: 241
23. Nishizawa M, Matsue T, Uchida I (1993) Sens Actuators B13–14: 53
24. Nishizawa M, Matsue T, Uchida I (1993) J Electroanal Chem 353: 329
25. Shibuya M, Yamamura S, Matsue T, Uchida I (1995) Chem Lett: 749
26. JCPDS Powder Diffraction File (1985) 35–782
27. Goodenough JB (1971) In: Reiss H (ed) Progress in solid state chemistry, vol 5. Pergamon, Oxford, pp 279
28. Many A, Goldstein Y, Grover NB (1965) Semiconductor surfaces. North Holland, Amsterdam, pp 210–255, 349–355
29. Myamlin VA, Pleskov YV (1967) Electrochemistry of semiconductors. Plenum, New York, pp 51–52, 135–140
30. Ooi K, Miyai Y, Katoh S, Maeda H, Abe M (1989) Langmuir 5: 150
31. Li W, Dahn JR (1995) J Electrochem Soc 142: 1742
32. Kanoh H, Feng Q, Miyai Y, Ooi K (1993) J Electrochem Soc 140: 3162
33. Kanoh H, Hirotsu T, Ooi K (1996) J Electrochem Soc 143: 905